

Supporting Information

Replacing the non-polarized C=C bond with an isoelectronic polarized B-N unit for the design and development of smart materials

Kalluvettukuzhy K. Neena and Pakkirisamy Thilagar*

Department of Inorganic and Physical Chemistry, Indian Institute of Science, Bangalore -560012, India.

Ph. No: +91-080-2293 3353 *Fax:* +91-80-2360 1552 **E-mail:* thilagar@ipc.iisc.ernet.in

NMR Spectral Characterizations

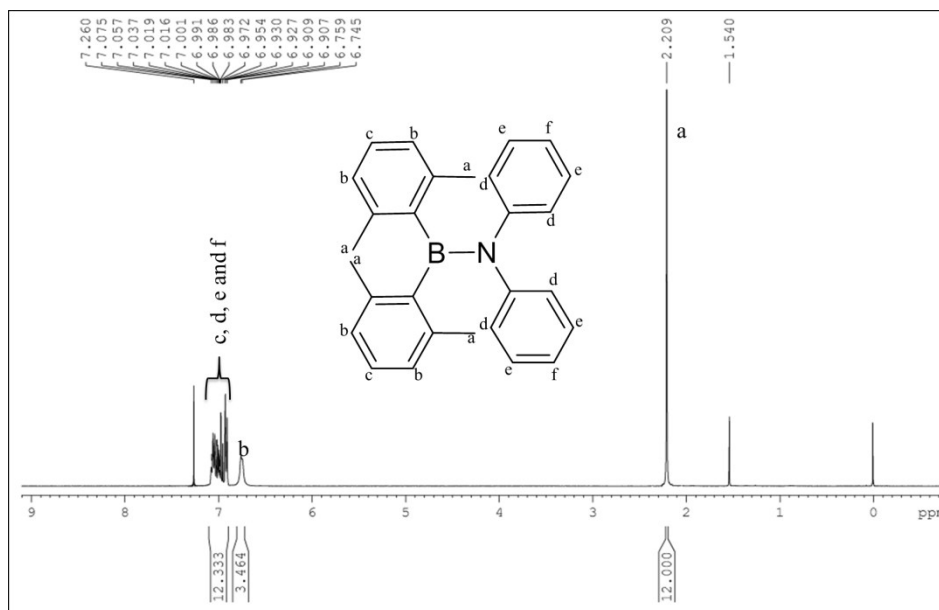


Figure S1. ^1H NMR spectrum of compound **1** ($\delta = 1.54$ ppm corresponds to H_2O in CDCl_3).

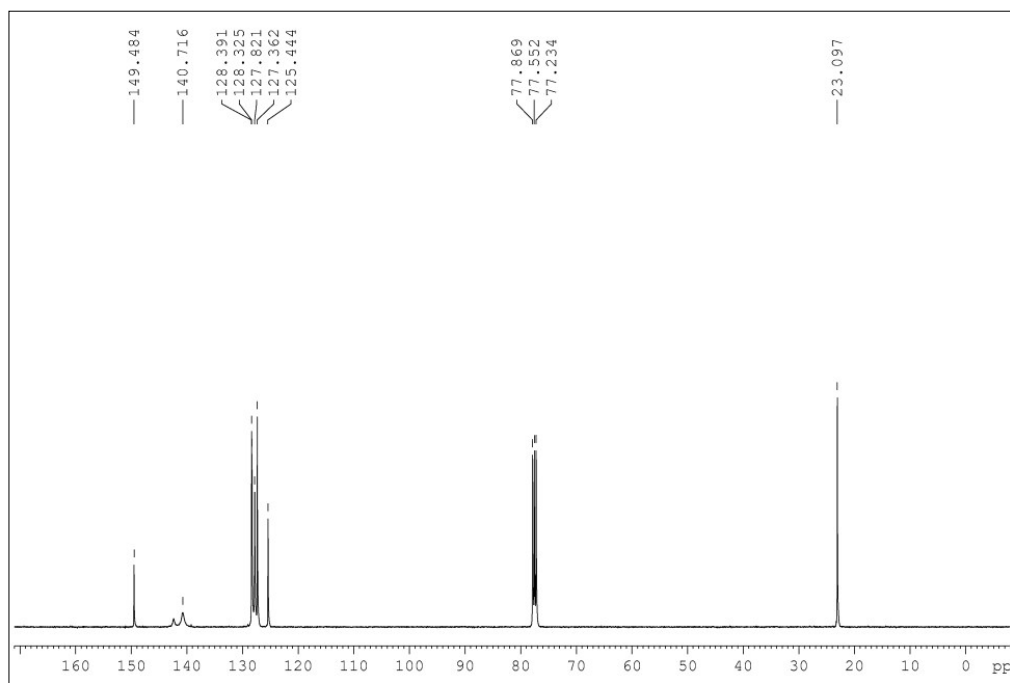


Figure S2. ^{13}C NMR spectrum of compound **1**



Figure S3. ^1H NMR spectrum of compound **2** ($\delta = 1.54$ ppm corresponds to H_2O in CDCl_3)

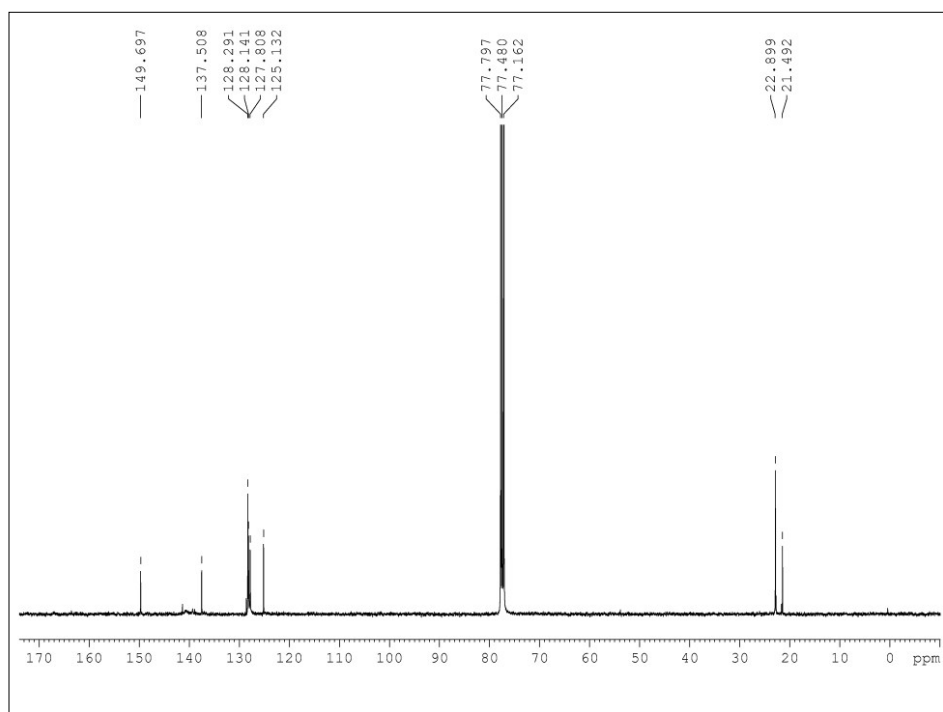


Figure S4. ^{13}C NMR spectrum of compound **2**

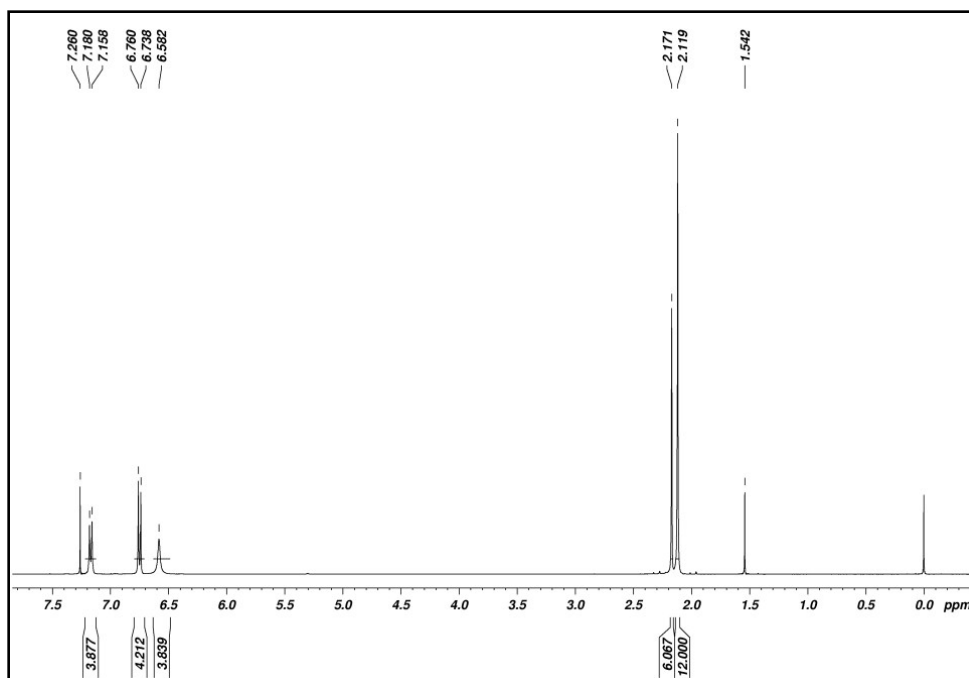


Figure S5. ^1H NMR spectrum of compound **2a** ($\delta = 1.54$ ppm corresponds to H_2O in CDCl_3)

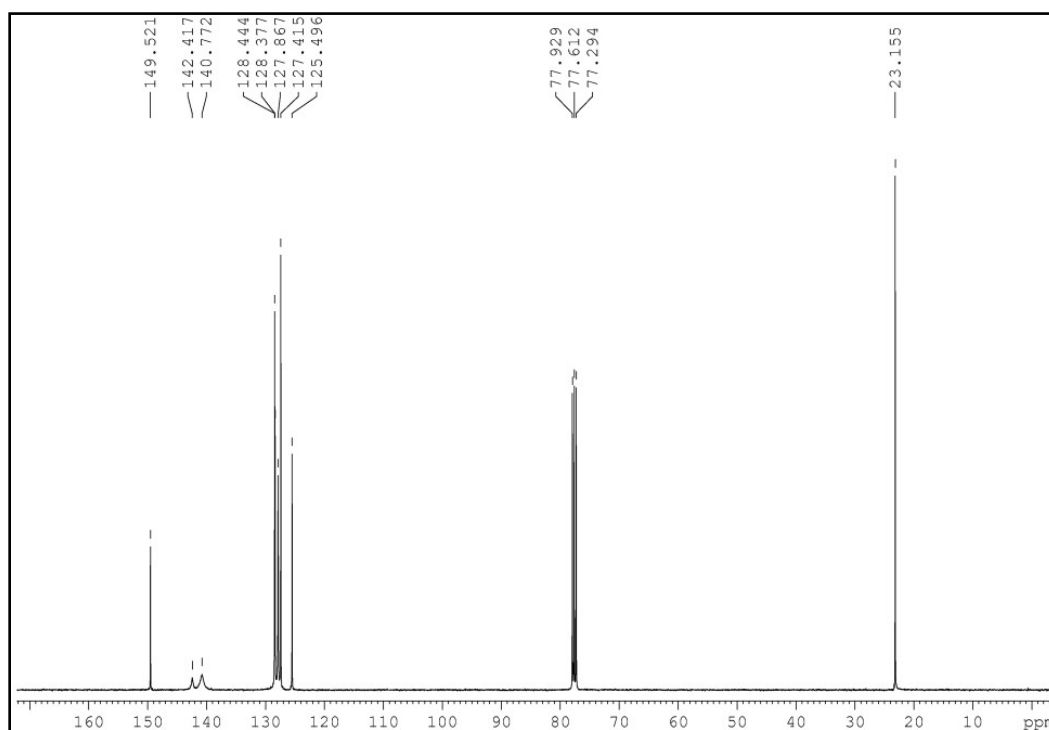


Figure S6. ^{13}C NMR spectrum of compound **2a**

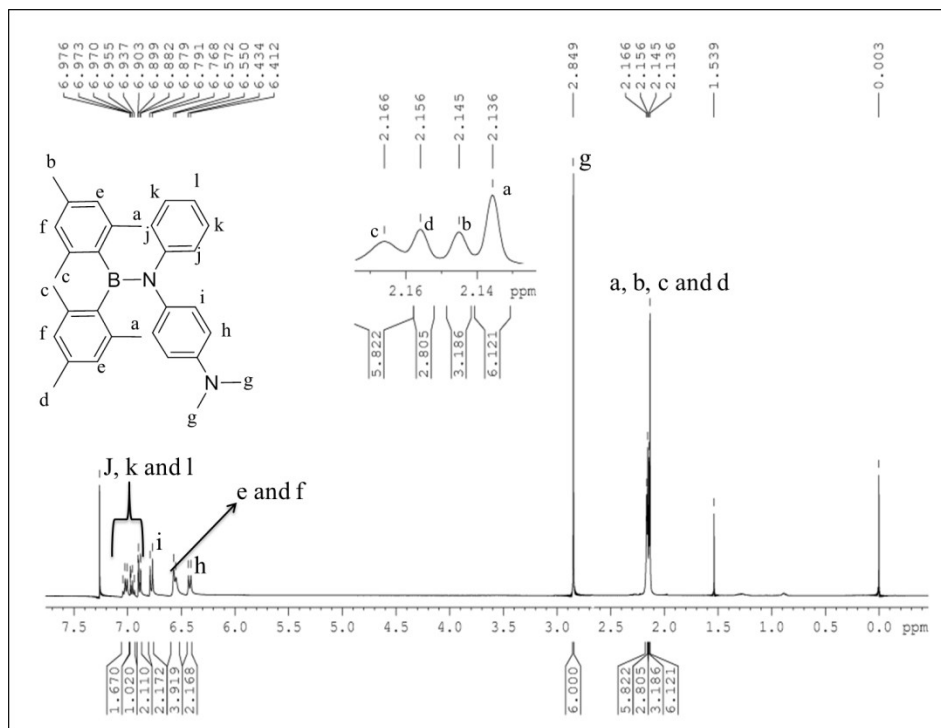


Figure S7. ¹H NMR spectrum of compound 3 ($\delta = 1.54$ ppm corresponds to H₂O in CDCl₃)

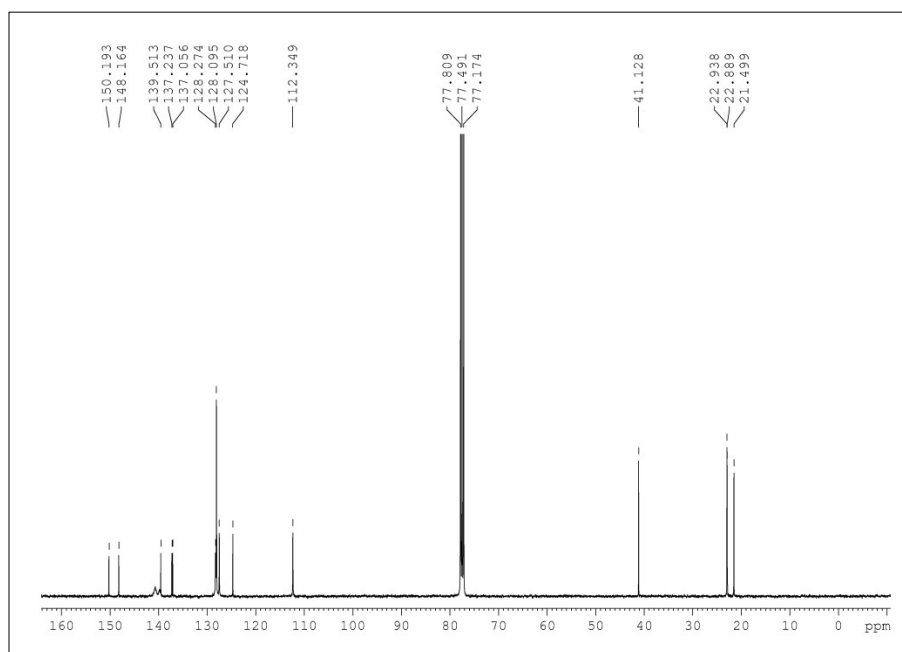


Figure S8. ¹³C NMR spectrum of compound 3

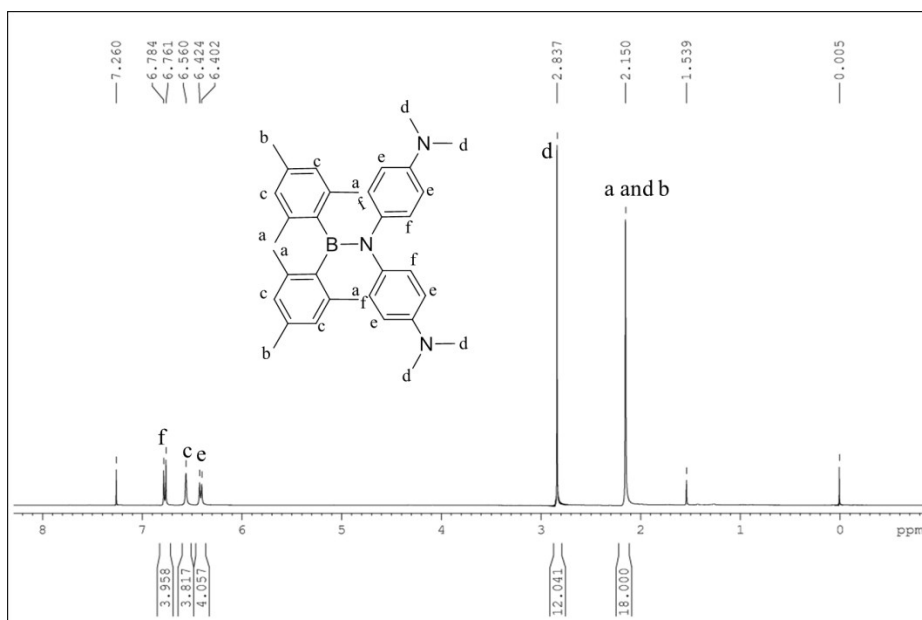


Figure S9. ^1H NMR spectrum of compound 4 ($\delta = 1.54$ ppm corresponds to H_2O in CDCl_3)

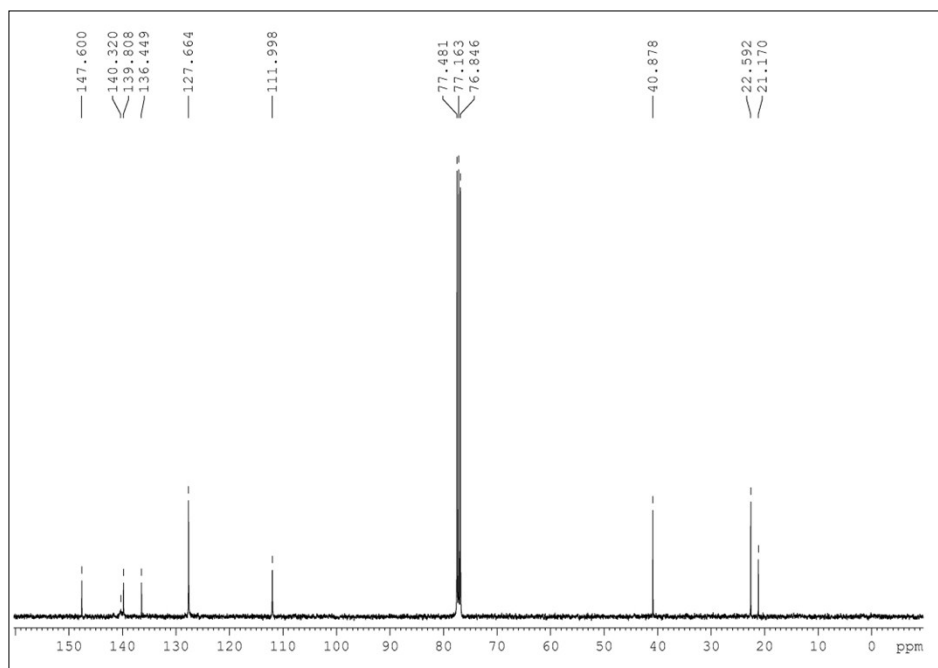


Figure S10. ^{13}C NMR spectrum of compound 4

Mass Spectral Characterization

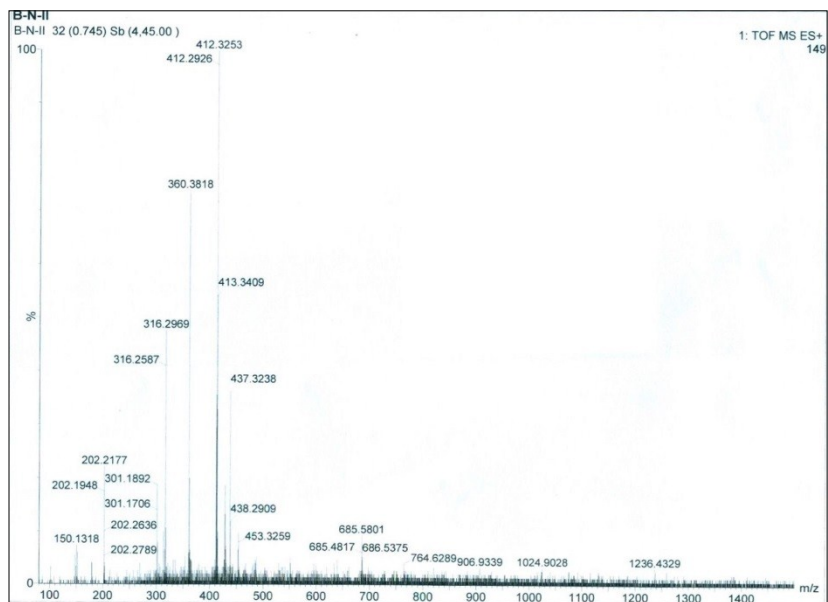


Figure S11. HRMS of compound 1

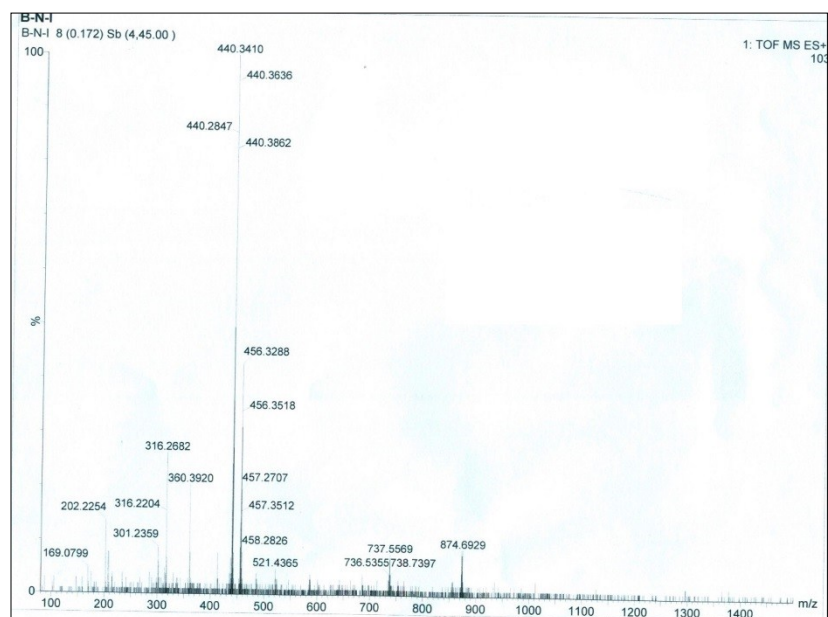


Figure S12. HRMS of compound 2

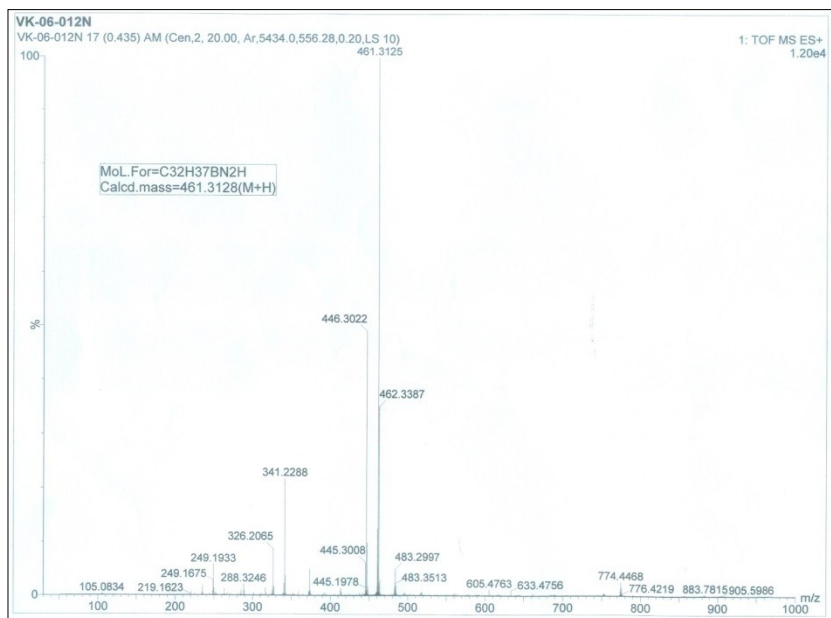


Figure S13. HRMS of compound 3

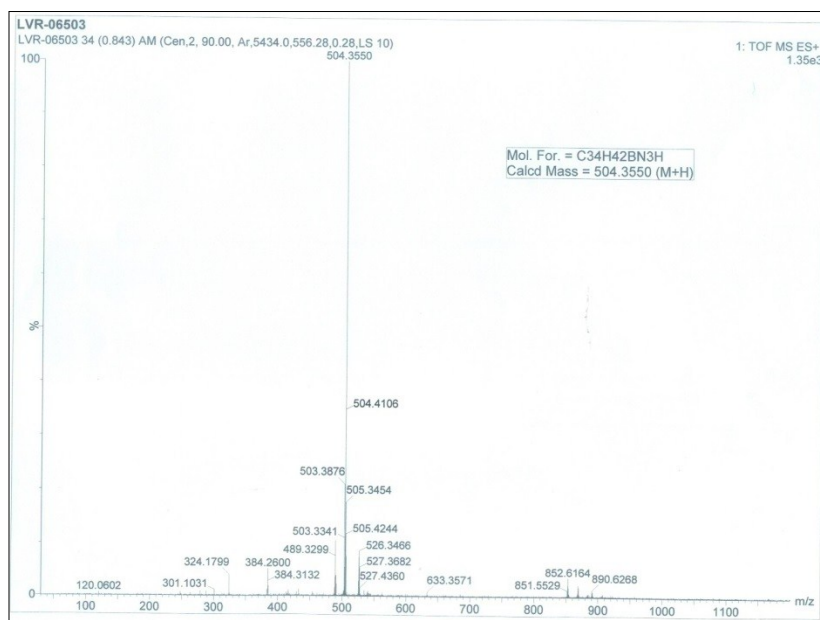


Figure S14. HRMS of compound 4

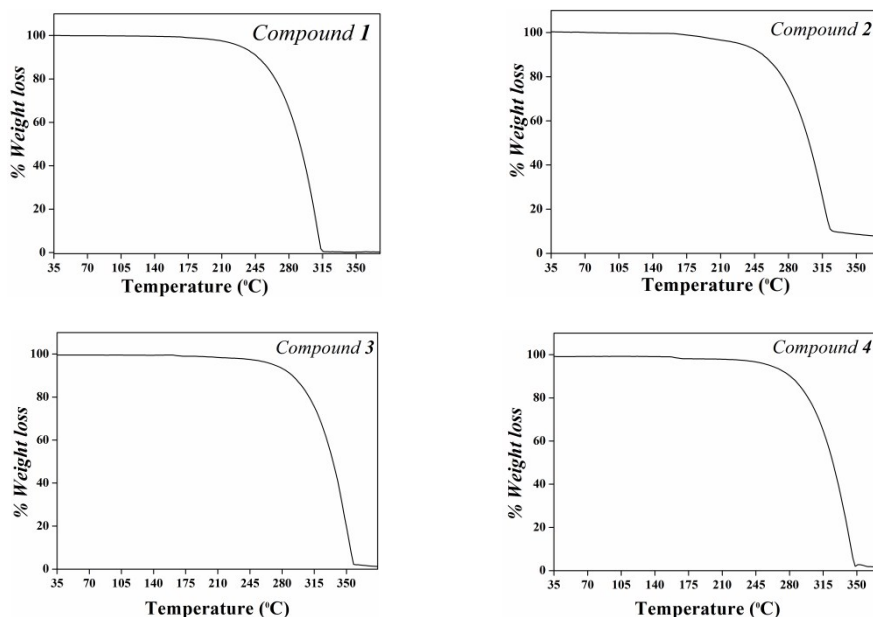


Figure S15. Thermo gravimetric traces of compounds **1**, **2**, **3** and **4**.

Optical Spectra of compounds **1**, **2**, **3** and **4**

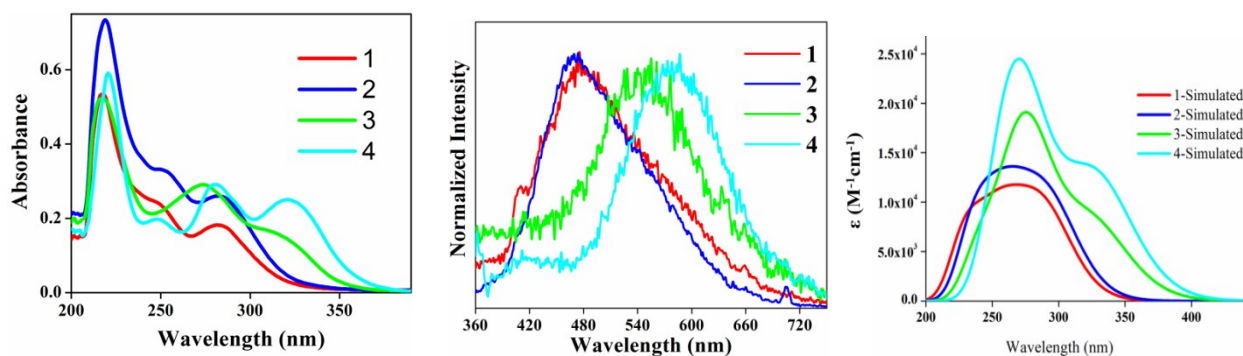


Figure S16. Absorption (right), emission (middle) spectra of compounds **1**, **2**, **3** and **4** in THF solvent (conc. 10^{-5} M, $\lambda_{\text{ex}} = 320$ nm for **1** and **2** and $\lambda_{\text{ex}} = 350$ nm for **3** and **4** respectively) and simulated absorption spectra from TD-DFT calculations (left). (Quantum yield in solution were calculated with respect to anthracene ($\phi_{\text{F}} = 27$ % in EtOH) and was found to be 0.2 %, 0.3 %, 0.03 %, 0.01 % respectively for **1**, **2**, **3** and **4**).

Table S1. Summary of dominant electronic transitions of compounds **1**, **2**, **3** and **4** obtained from TD-DFT calculations.

Compound	Excited State	E/eV	E/nm	f	Dominant transitions (percent contribution)
1	1	4.261	291.01	0.205	HOMO ->LUMO (97%)
	2	4.508	275.03	0.002	HOMO-1 ->LUMO (94%)
	3	4.624	268.11	0.026	HOMO-3 ->LUMO (56%)
	4	4.641	267.16	0.019	HOMO-2 ->LUMO (55%)
	5	4.716	262.90	0.047	HOMO ->LUMO+1 (65%)
	6	4.832	256.60	0.111	HOMO ->LUMO+2 (64%)
2	1	4.193	295.70	0.207	HOMO ->LUMO (98%)
	2	4.496	275.76	0.048	HOMO-2 ->LUMO (95 %)
	3	4.500	275.49	0.005	HOMO-1 ->LUMO (93%)
	4	4.623	268.22	0.019	HOMO-3 ->LUMO (82%)
	5	4.664	265.81	0.063	HOMO ->LUMO+1 (62%)
	6	4.768	260.06	0.099	HOMO ->LUMO+2 (61%)
3	1	3.787	327.40	0.180	HOMO ->LUMO (98%)
	2	4.212	294.37	0.045	HOMO ->LUMO+1 (92%)
	3	4.442	279.11	0.239	HOMO ->LUMO+2 (80%)
	4	4.507	257.07	0.008	HOMO-1 ->LUMO (57%)
	5	4.540	273.09	0.043	HOMO-2 ->LUMO (63%)
	6	4.577	270.89	0.079	HOMO-1 ->LUMO+1 (23%)
4	1	3.745	331.07	0.275	HOMO ->LUMO (99%)
	2	4.066	304.94	0.052	HOMO ->LUMO+1 (94%)
	3	4.263	290.84	0.042	HOMO-1 ->LUMO (87%)
	4	4.418	280.67	0.202	HOMO ->LUMO+2 (81%)
	5	4.441	279.18	0.008	HOMO ->LUMO+4 (86%)
	6	4.526	273.92	0.104	HOMO ->LUMO+3 (91%)

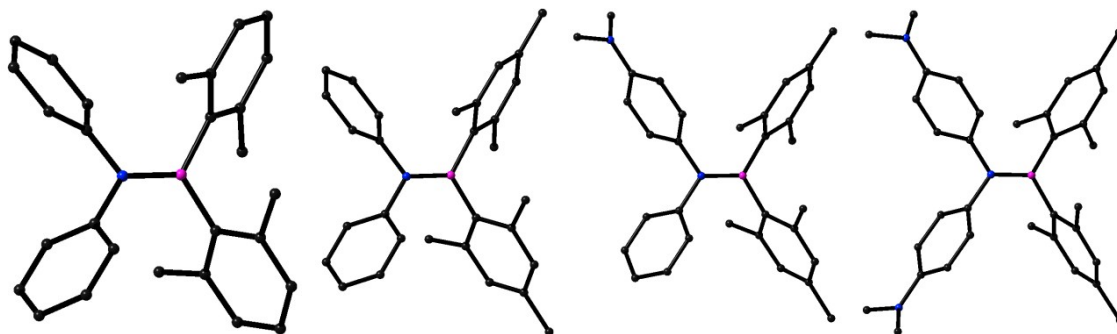


Figure S17. Ground state DFT optimized structures of **1**, **2**, **3** and **4** (left to right) from the ground state DFT optimized structures (Atom color codes: C-black, N-blue, B-purple, hydrogen atoms are removed for clarity).

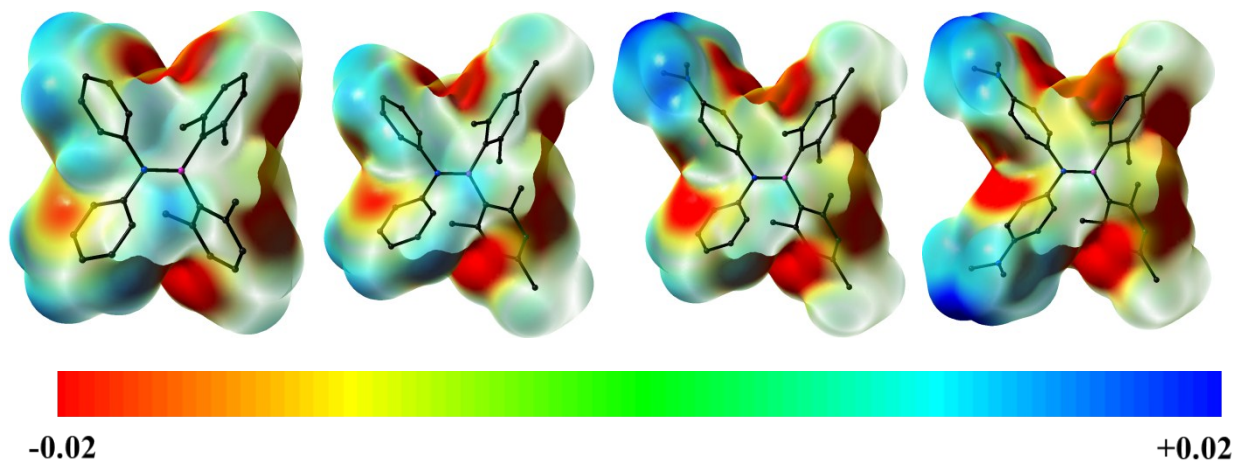


Figure S18. Electrostatic potential energy surface diagrams of **1**, **2**, **3** and **4** (left to right) from the ground state DFT optimized structures (Atom color codes: C-black, N-blue, B-purple, hydrogen atoms are removed for clarity, isovalue = 0.0004).

Solvent dependent absorption and emission spectra of 1, 2, 3 and 4

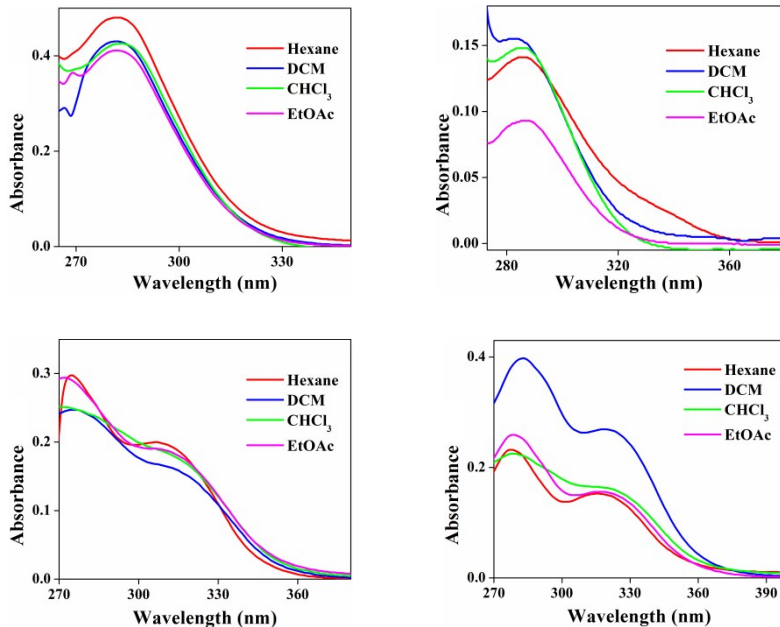


Figure S19. Absorption spectra of **1** (top left), **2** (top right), **3** (bottom left) and **4** (bottom right) in different solvents (Conc. 10⁻⁵ M).

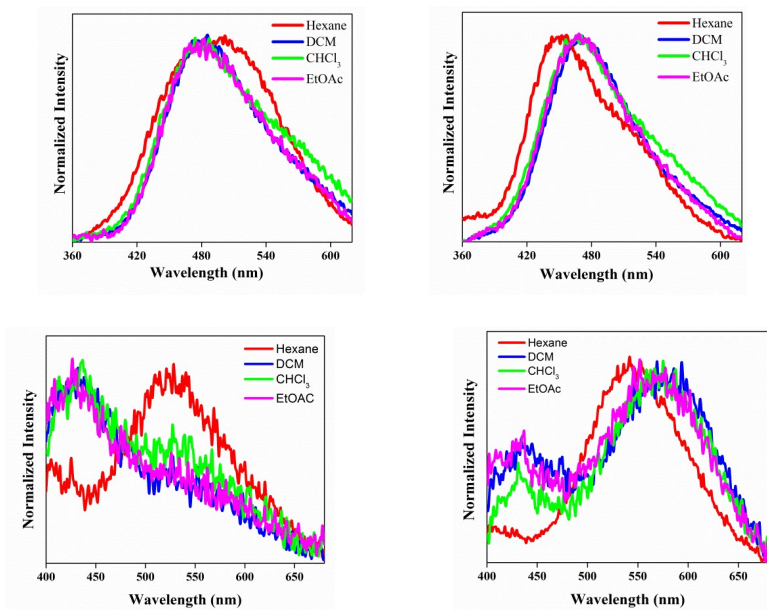


Figure S20. Normalized emission spectra of **1** (top left), **2** (top right), **3** (bottom left) and **4** (bottom right) in different solvents, (Conc. 10⁻⁵ M, λ_{ex} = 320 nm for **1** and **2** and λ_{ex} = 350 nm for **3** and **4** respectively).

Table S2. Luminescence data of **1**, **2**, **3** and **4** in different Solvents (Conc. 10^{-5} M)

	Solvent	λ_{abs} (nm)	λ_{em} (nm)	ν (cm^{-1})
1	Hexane	282	490	15053
	DCM	282	483	14757
	CHCl_3	282	484	14800
	EtOAc	282	485	14842
2	Hexane	286	452	12841
	DCM	286	469	13643
	CHCl_3	286	471	13734
	EtOAc	287	470	13567
3	Hexane	313	525	12901
	DCM	313	<i>n.d</i>	<i>n.d</i>
	CHCl_3	313	<i>n.d</i>	<i>n.d</i>
	EtOAc	313	<i>n.d</i>	<i>n.d</i>
4	Hexane	323	544	12577
	DCM	323	579	13689
	CHCl_3	323	575	13568
	EtOAc	323	571	13447

**n.d*= not determined

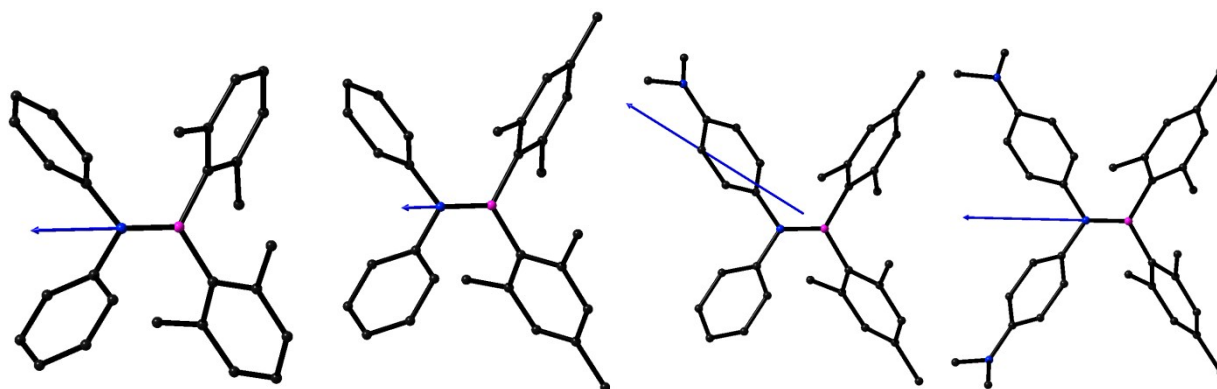
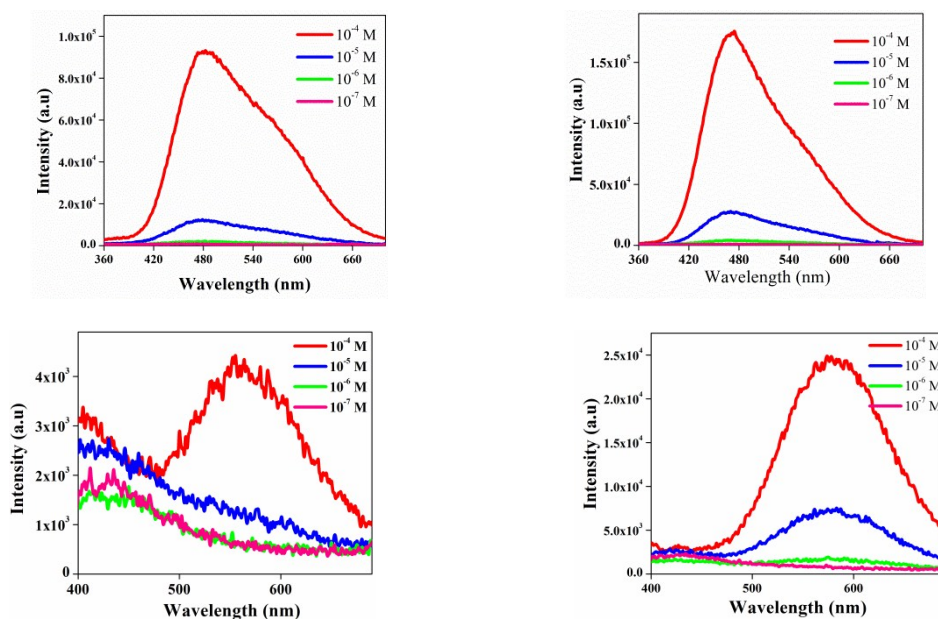


Figure S21. Orientation of ground state dipole moment of **1**, **2**, **3** and **4** (left to right) from the DFT optimized structures (Atom color codes: C-black, N-blue, B-purple, hydrogen atoms are removed for clarity).

Table S3. Ground state and excited state dipole moment values of **1**, **2**, **3** and **4**

Compound No.	Dipole moment (Debye)		
	Ground state (μ_g) ^a	Excited state (μ_e) ^b	$\Delta\mu = \mu_e - \mu_g$
1	1.61	6.59	4.98
2	1.15	6.79	5.64
3	3.39	<i>n.d</i>	<i>n.d</i>
4	4.38	10.39	6.01

a. obtained from DFT calculations; b. $\Delta\nu^s = (2\Delta\mu^2/hca_0^3) f(X) + A$, where $\Delta\mu$ is the electric dipole moment change upon electronic transition and h , c , a_0 , and A are the Planck's constant ($h = 6.626 \times 10^{-34}$ J s), speed of light ($c = 2.99 \times 10^8$ m/s), Onsager radius of fluorophore and a constant. **n.d*= not determined.

**Figure S22.** Emission spectra of **1** (top left), **2** (top right), **3** (bottom left) and **4** (bottom right) at different concentrations in THF solvent (λ_{ex} = 320 nm for **1** and **2** and 350 nm for **3** and **4**).

Single crystal X-ray diffraction studies

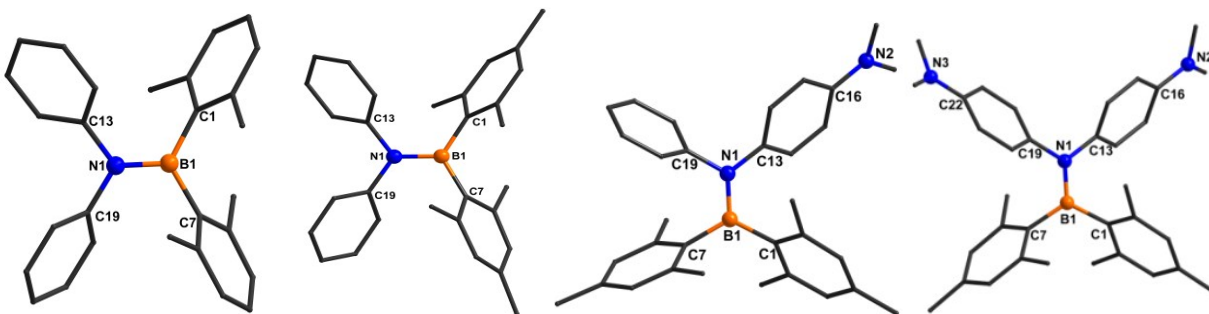
Table S4. Crystallographic refinement data of compounds **1**, **2**, **3** and **4**

	1	2	3	4
Empirical formula	C ₂₈ H ₂₈ B ₁ N ₁	C ₃₀ H ₃₂ B ₁ N ₁	C ₃₂ H ₃₇ B ₁ N ₂	C ₃₄ H ₄₂ B ₁ N ₃
Formula weight	389.32	417.38	460.46	503.52
Temperature(K)	100(2)	100(2)	298(2)	100(2)
Wavelength (Å)	0.71073	0.71073	0.71073	0.71073
Crystal system	Monoclinic	Monoclinic	Monoclinic	Monoclinic
Space group	<i>P2₁/c</i>	<i>P2₁/c</i>	<i>P2₁/c</i>	<i>P2₁/c</i>
a/ Å	9.224(5)	9.418(4)	17.373(28)	20.500(12)
b/ Å	15.412(8)	15.613(6)	9.361(14)	12.535(7)
c/ Å	16.217(8)	16.741(7)	18.579(29)	14.258(8)
α/°	90.0	90.0	90.0	90.0
β/°	99.8(14)	94.8(11)	113.2(7)	105.8(2)
γ/°	90	90	90	90
V/Å ³	2272.0(2)	2452.9(17)	2775.9(91)	3524.5(21)
Crystal size (mm ³)	0.10 x 0.08 x 0.05	0.1 x 0.09 x 0.07	0.20 x 0.09 x 0.07	0.12x0.08x0.06
Z	4	4	4	4
Density(g cm ⁻³)	1.138	1.13	1.10	0.95
Final R [I>2s(I)] [a], [b]	R1 = 0.0675, wR2 = 0.1858	R1 = 0.0662, wR2 = 0.1914	R1 = 0.049, wR2 = 0.121	R1 = 0.124, wR2 = 0.394
R (all data) ^{[a], [b]}	R1 = 0.0889, wR2 = 0.2023	R1 = 0.0969, wR2 = 0.2148	R1 = 0.089, wR2 = 0.137	R1 = 0.159, wR2 = 0.413
Collected reflns	71456	68641	40669	31085
Unique reflns	3987	4295	5468	3177
Theta range for data collection	3.06 to 25.00	3.13 to 25.00	1.3 to 26.00	3.0 to 26.0
Absorption coefficient	0.064 mm ⁻¹	0.064 mm ⁻¹	0.063 mm ⁻¹	0.054
Goodness-of-fit on F ²	1.042	0.962	0.966	1.75
CCDC No.	1453219	1453220	1453221	1453222

** Unidentified solvent molecule in the crystal lattice of compound **4** was removed by giving squeeze command

$${}^{[a]}R_1 = \Sigma \left| |F_o| - |F_c| \right| / \Sigma |F_o|, {}^{[b]}wR_2 = [\Sigma\{w(F_o^2 - F_c^2)^2\} / \Sigma\{w(F_o^2)^2\}]^{1/2}$$

Table S5. Selected bond lengths (Å), bond angles and dihedral angles (°) for **1**, **2**, **3** and **4**



Molecular Structures of compounds **1**, **2**, **3** and **4** (left to right) with atom numbering schemes.

	1	2	3	4
B1-N1	1.423(3)	1.429(3)	1.419(2)	1.416(7)
B1-C1	1.591(3)	1.587(3)	1.587(2)	1.586(5)
B1-C7	1.600(3)	1.587(3)	1.590(2)	1.586(5)
N1-C13	1.449(3)	1.443(3)	1.442(2)	1.455(4)
N1-C19	1.444(3)	1.443(3)	1.443(2)	1.455(4)
N2-C16	-	-	1.380(2)	1.396(5)
N3-C22	-	-	-	1.396(5)
∠C1-B1-C7	121.93(19)	122.6(2)	122.4(1)	119.5(4)
∠N1-B1-C1	120.26(19)	119.9(2)	120.2(1)	120.3(5)
∠N1-B1-C7	117.8(2)	117.5(2)	117.4(1)	120.3(5)
∠C13-N1-C19	112.77(17)	113.8(2)	113.2(1)	114.2(3)
∠B1-N1-C13	124.39(18)	123.5(2)	125.1(1)	122.9(4)
∠B1-N1-C19	122.84(18)	122.7(2)	121.6(1)	122.9(4)
∠C1-B1-N1-C13	-10.9(3)	-12.2(3)	-14.8(2)	23.7(7)
∠C7-B1-N1-C19	-10.7(3)	-9.5(3)	-10.1(2)	23.7(7)
∠C1-B1-N1-C19	168.8(2)	169.3(2)	168.2(1)	-156.3(4)
∠C7-B1-N1-C13	169.6(2)	169.0(2)	166.8(1)	-156.3(4)

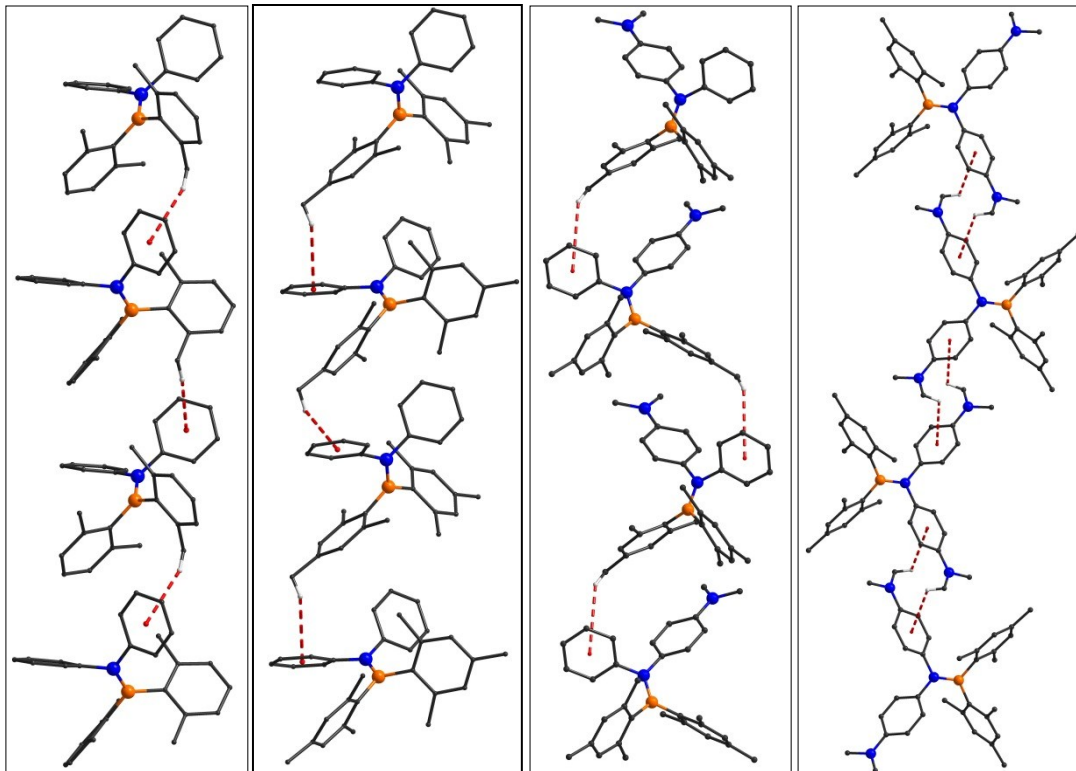


Figure S23. Intermolecular interaction diagrams of compound **1** (left), **2** (middle left), **3** (middle right) and **4** (right). (Hydrogen atoms are omitted for clarity).

Aggregation Induced Emission Studies

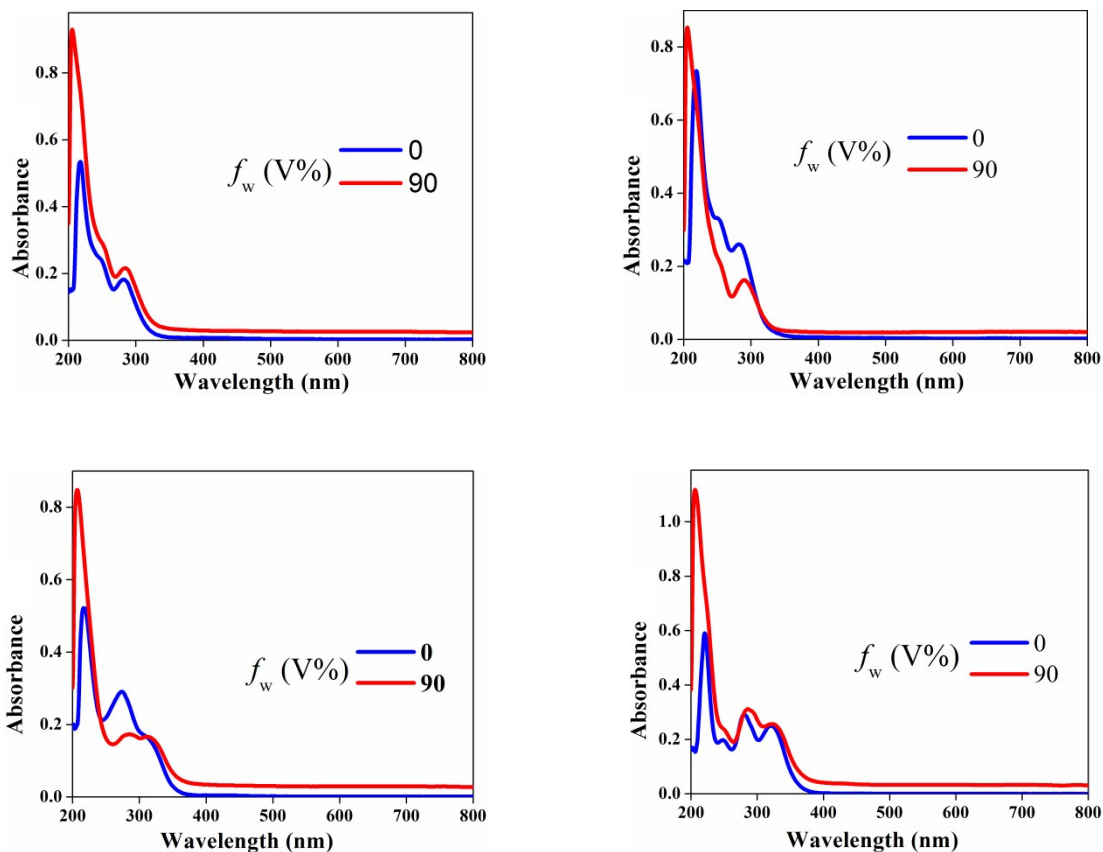
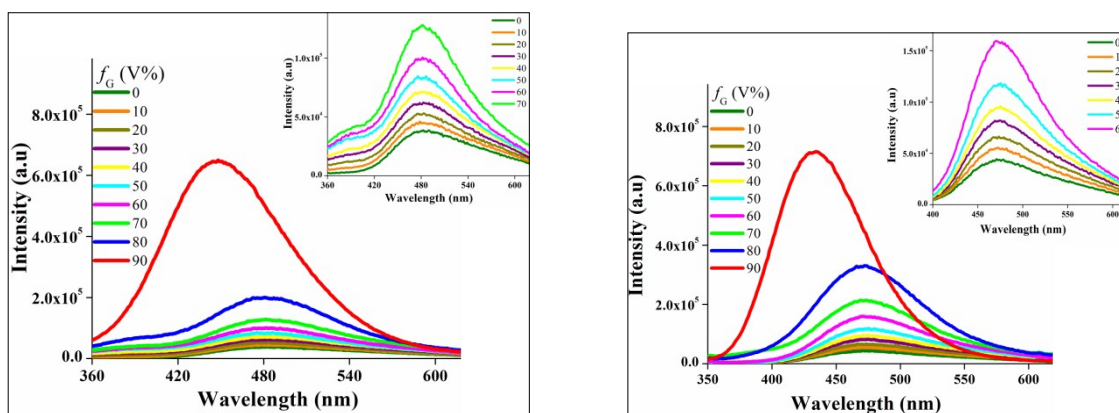


Figure S24. Absorption spectra of **1** (top left), **2** (top right), **3** (bottom left) and **4** (bottom right) in THF and 1:9 THF-H₂O mixture (Conc. 10⁻⁵ M, the level-off tails in the absorption spectra of 1:9 THF-water mixture is due to scattering of light by particles in solution, which confirms the formation of nano-aggregates.)



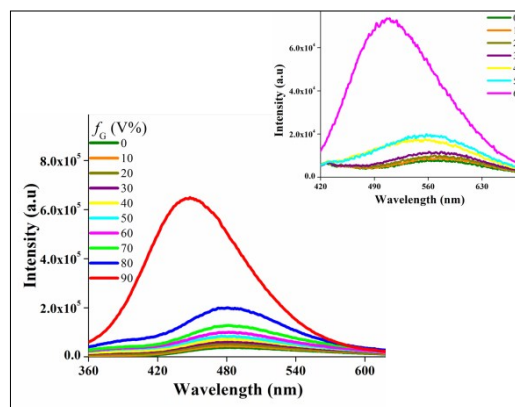
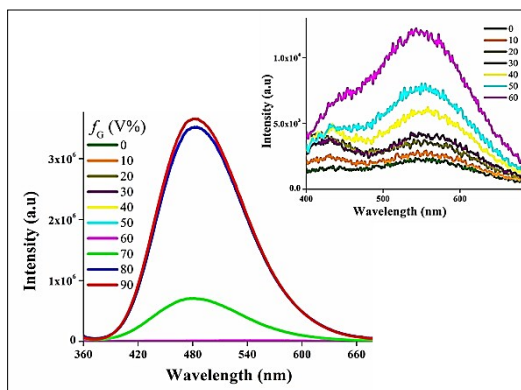
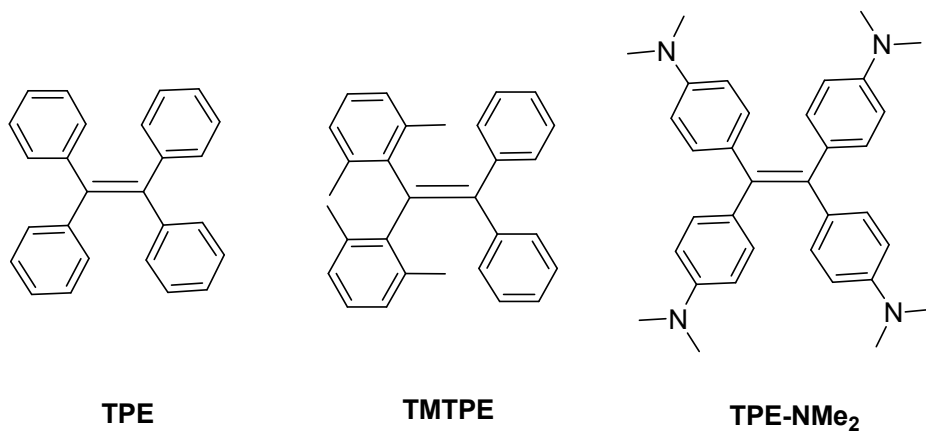


Figure S25. PL spectra of **1** (top left) **2** (top right), **3** (bottom left) and **4** (bottom right) respectively in MeOH/Glycerol mixtures with different glycerol fraction, f_G (V%) (Conc. 10^{-4} M, λ_{ex} = 320 nm for **1** and **2** and 350 nm for **3** and **4**, and inset shows the PL spectra at lower glycerol fractions 0 to 60).

Table S6. Comparison of PL data of **1**, **2**, **3** and **4** in solution and aggregated state (Conc. 10^{-4} M) with the tetraarylethene derivatives such as TPE, TMTPE and TPE-NMe₂ (Conc. 10^{-5} M).



	AIE studies			Viscochromism		
	F_w (V%)	λ_{em}	I/I ₀	f_G (V%)	λ_{em}	I/I ₀
TPE ^{1a}	90	-	69	-	-	-
TMTPE ^{1b}	90	-	Non-AIE active	-	-	-
TPE-NMe₂ ^{1c}	90		64	-	-	-
1	0	487		0	483	
	90	464	18	90	448	17
2	0	470		0	471	
	90	449	14	90	434	16
3	0	559		0	554	
	90	489	391	90	489	1510
4	0	581		0	580	
	90	504	134	90	497	455

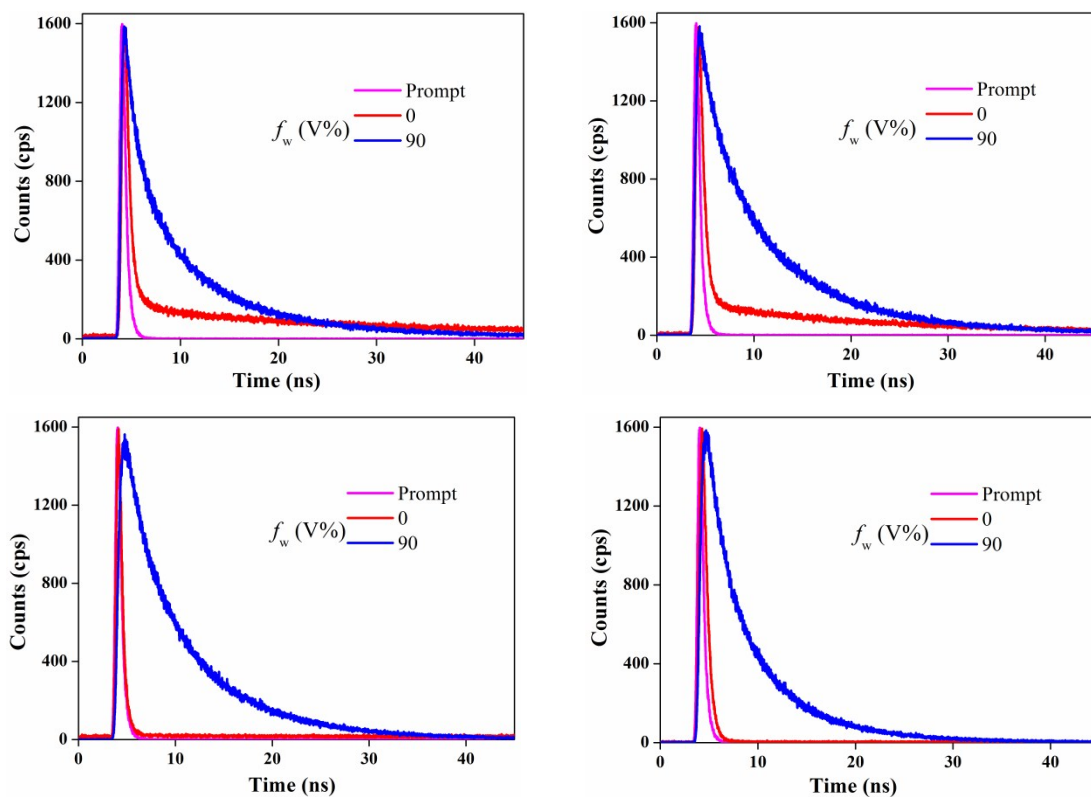


Figure S26. Time resolved fluorescence decay profile of **1** (top left), **2** (top right), **3** (bottom left), and **4** (bottom right) in THF and 1:9 THF-water mixture (Conc. 10^{-4} M, $\lambda_{\text{exc}} = 340$ nano-LED).

Table S7. Time resolved fluorescence decay data of **1**, **2**, **3** and **4** in THF and 1:9 THF-water mixture (Conc. 10^{-4} M, $\lambda_{\text{exc}} = 340$ nano-LED).

Compound	H ₂ O (%)	τ_1 (ns)	A ₁	τ_2 (ns)	A ₂	Mean life time ($\langle \tau \rangle = A_1\tau_1 + A_2\tau_2$)	χ^2
1	0	0.22	0.30	20.99	0.70	14.76	1.2
	90	1.48	0.13	7.42	0.85	6.50	1.0
2	0	0.29	0.37	16.39	0.63	10.43	1.1
	90	1.94	0.14	8.62	0.86	7.68	1.2
3	0	0.09	0.79	0.6	0.21	0.20	1.2
	90	3.20	0.24	8.29	0.76	7.07	1.0
4	0	0.30	0.68	0.61	0.32	0.40	1.1
	90	2.16	0.28	6.49	0.72	5.28	1.1

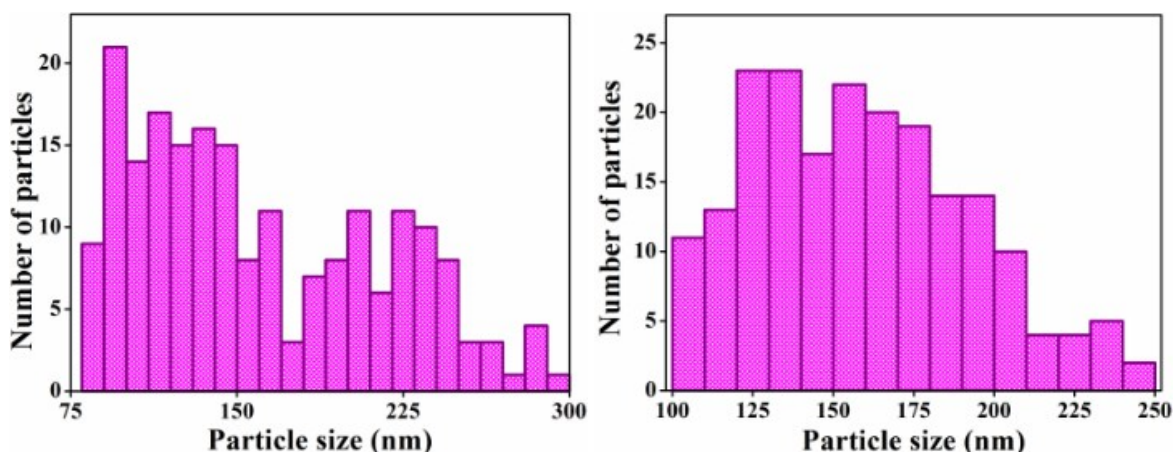


Figure S27. Particle size distribution pattern of compounds **3** (left) and **4** (right) obtained from TEM image by counting 200 particles using digital micrograph demo software and then plotting in origin, the average particle size was found to be 160.284 ± 55.39 nm, 158.578 ± 33.8 nm for **3** and **4** respectively.

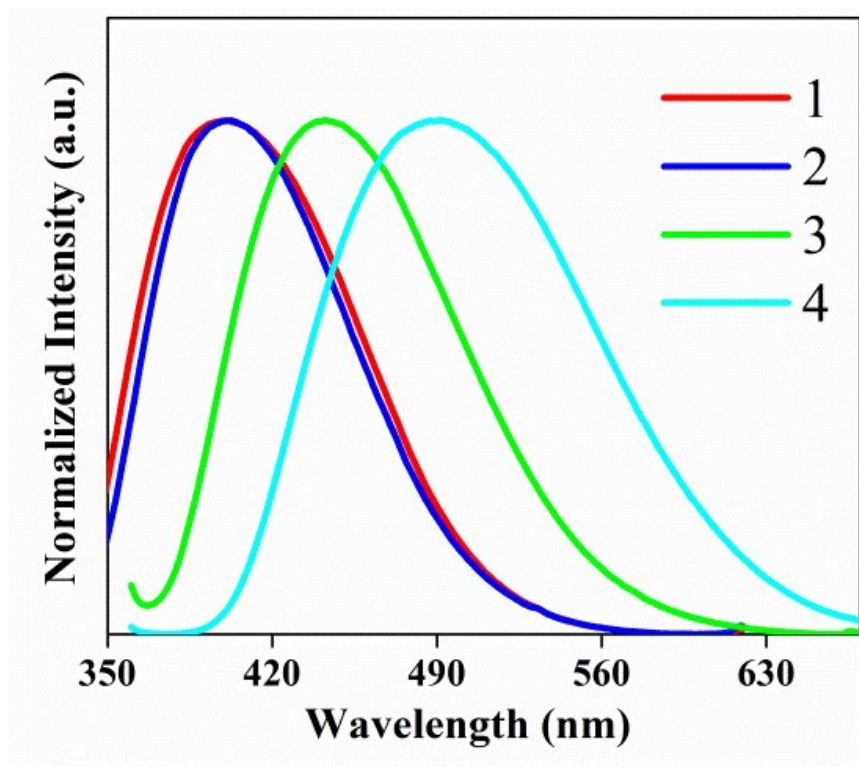


Figure S28. Solid state emission spectra (normalized) of **1**, **2**, **3** and **4** ($\lambda_{\text{ex}} = 320$ nm for **1** and **2** and $\lambda_{\text{ex}} = 350$ nm for **3** and **4**).

Table S8. Solid state fluorescence data of **1**, **2**, **3** and **4** ($\lambda_{\text{ex}} = 320$ nm for **1** and **2** and 350 nm for **3** and **4** for PL measurements **and** $\lambda_{\text{ex}} = 340$ nano-LED for TRF measurements).

	λ	ϕ_F (%)	τ (ns)	χ^2	$K_r \times 10^9$ (S ⁻¹) ^a	$K_{nr} \times 10^9$ (S ⁻¹) ^a
1	400	11.4	1.27	1.16	0.089	0.698
2	400	13.4	1.05	1.01	0.128	0.825
3	443	48.4	5.41	0.99	0.089	0.095
4	490	25.1	5.43	1.11	0.046	0.138

^aFollowing equations have been used for the calculation of K_r and K_{nr} ; $\{\phi_F = k_r/(k_r+k_{nr})\}$ and $\{\tau = 1/(k_r+k_{nr})\}$, where ϕ_F is the fluorescence quantum yield, τ is the average life time and k_r and k_{nr} are the radiative non-radiative (k_{nr}) decay rate constants, respectively.²

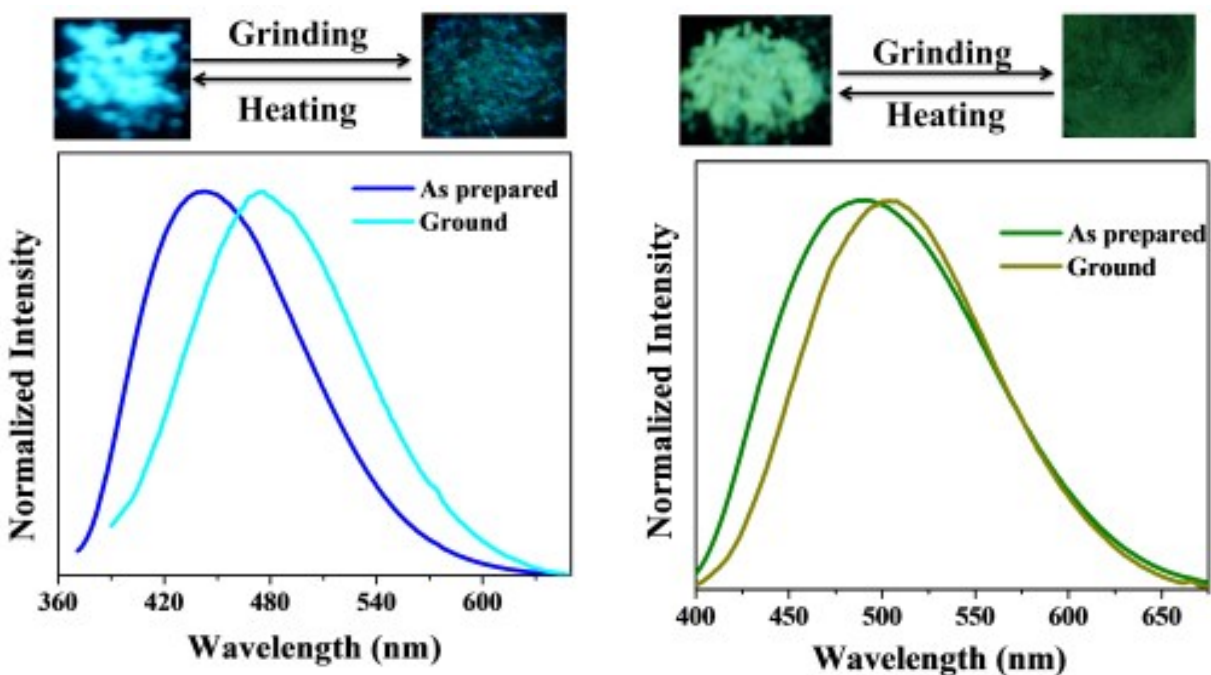


Figure S29. Solid state emission spectra (normalized) of as-prepared and ground samples of **3** (left) and **4** (right) ($\lambda_{\text{ex}} = 350$ nm) and the corresponding images of compounds taken under UV light illumination ($\lambda = 280$ -365 nm).

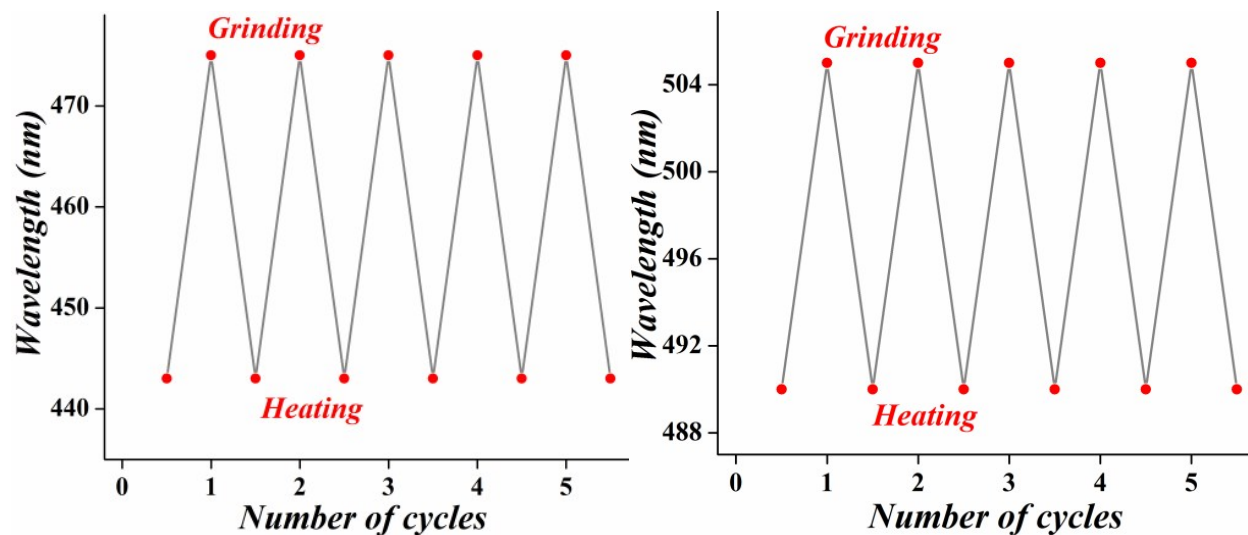


Figure S30. Reversible fluorescence responses of **3** (left) and **4** (right) over five successive cycles of grinding and annealing processes. ($\lambda_{\text{ex}} = 350\text{nm}$).

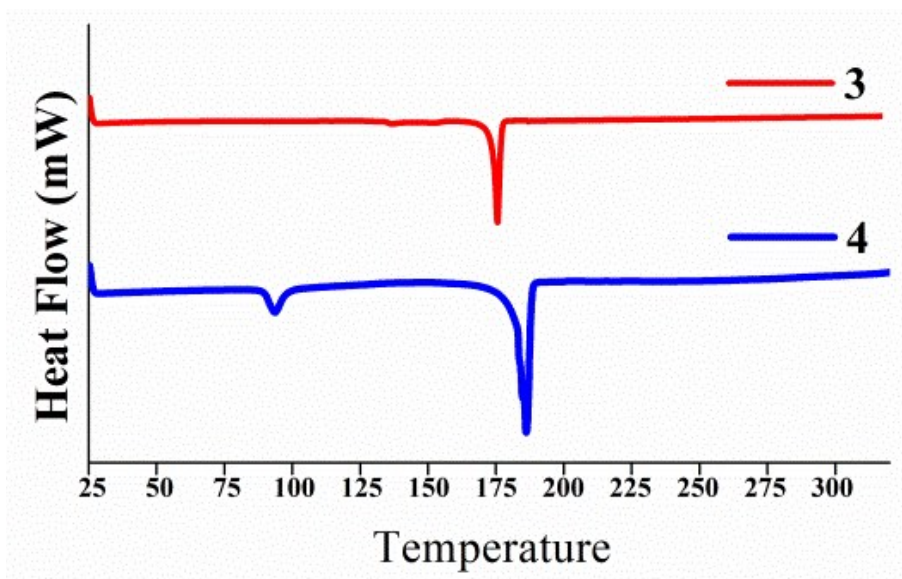


Figure S31. DSC traces of compounds **3** and **4**.

Detection of nitroaromatics

Reactivity of compounds **1-4** towards different nitroaromatic compounds/ nitroalkanes were carried out by titrating $100\ \mu\text{M}$ solution of compounds in 1:9 THF-water mixture with THF solution of nitroaromatic compounds/ nitroalkanes ($50\ \text{mM}$) in excess quantity. Picric

acid sensor studies were carried out by titrating 100 μM solution of compounds in 1:9 THF-water mixtures with aqueous solution of picric acid (50 mM). Emission spectral measurements were carried out gradually increasing the concentration of picric acid and spectra were collected 3 minutes after the addition of picric acid.

Fluorescence quenching efficiency for analytes were calculated by the following equation, $\eta = (I_0 - I) / I_0 \times 100$. Where, I_0 is the initial intensity of the sensors and I is the intensity after addition of analytes

Stern-Volmer plot was obtained by plotting relative fluorescence intensity (I/I_0) against picric acid concentration. Stern-Volmer constants (KSV) was obtained from the slope of the curve by fitting to the Stern-Volmer equation $I/I_0 = 1 + K_{sv}[X]$, where $[X]$ is the concentration of picric acid (1.5 equivalents).

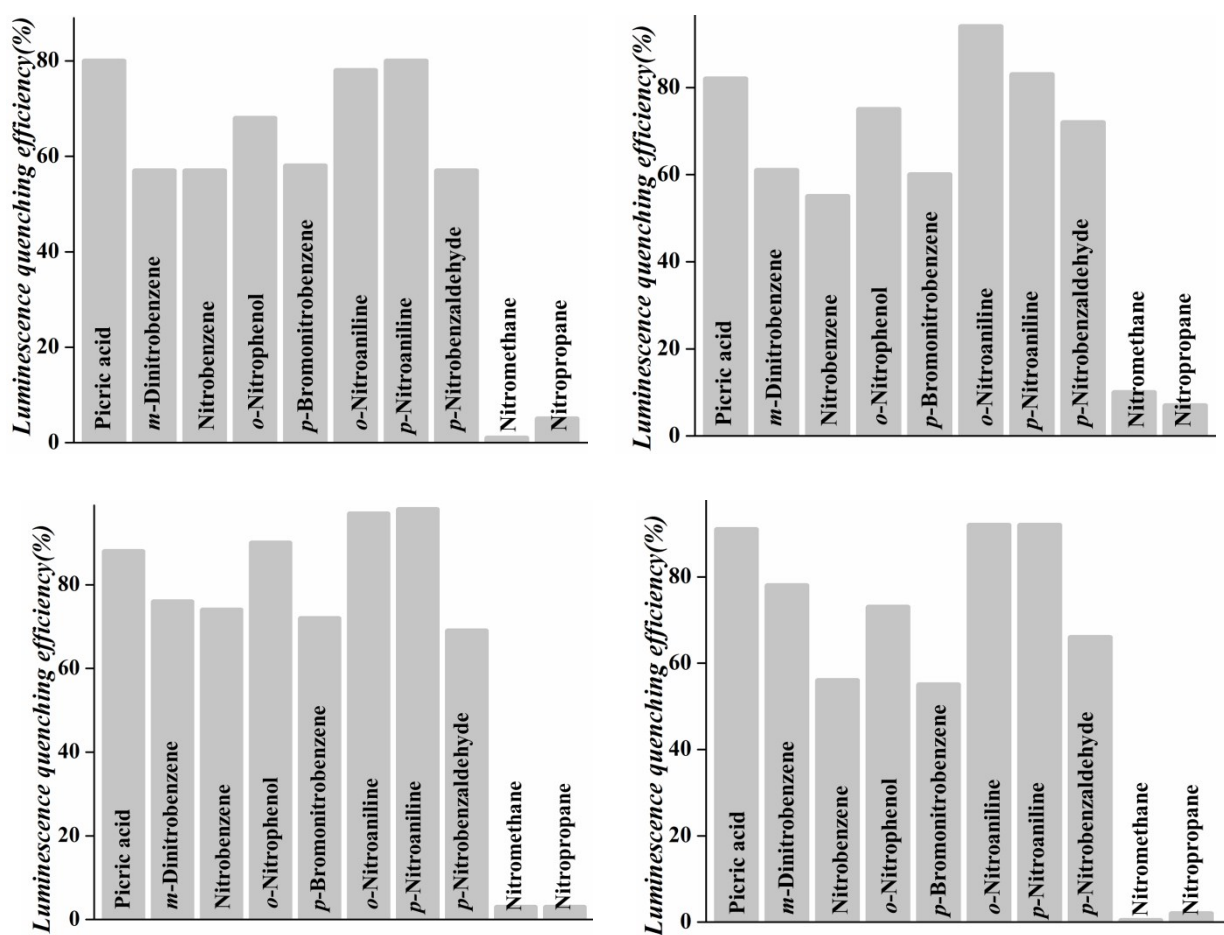


Figure S32. Plot showing reactivity of compounds **1** (top left), **2** (top right), **3** (bottom left), and **4** (bottom right), (100 μM in 1:9 THF-water mixture) with different nitroaromatics (2 equivalents) and nitroalkanes (4 equivalents).

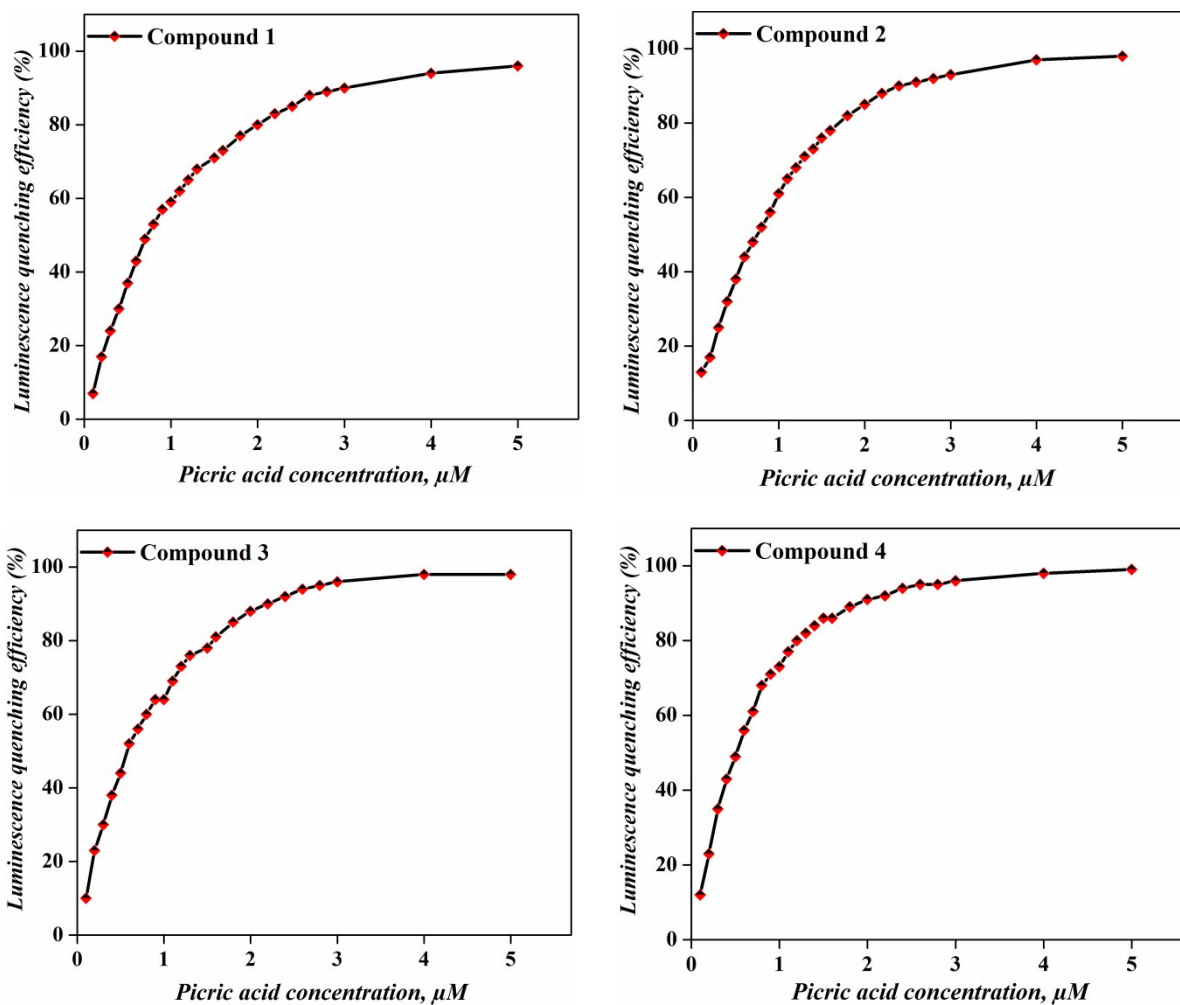


Figure S33. Luminescence quenching efficiency of compounds **1** (top left), **2** (top right), **3** (bottom left), and **4** (bottom right), (100 μM in 1:9 THF-water mixture) with increasing concentration of picric acid.

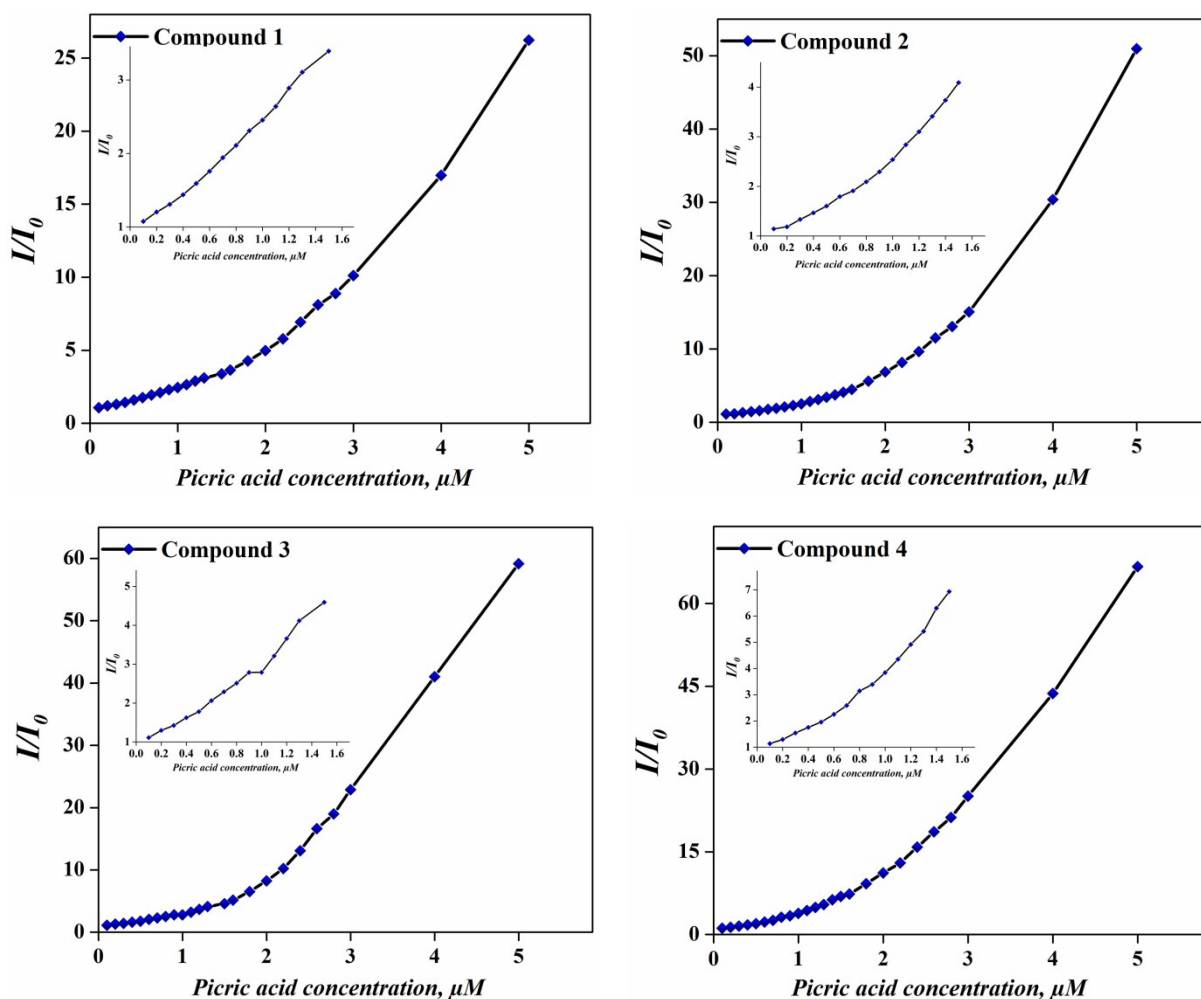


Figure S34. Stern-Volmer plots for the luminescence quenching of compounds **1** (top left), **2** (top right), **3** (bottom left), and **4** (bottom right), (100 μM in 1:9 THF-water mixture) with increasing concentration of picric acid and inset shows the corresponding Stern-Volmer plots at lower concentrations of picric acid.

References

- (a) G.-F. Zhang, Z.-Q. Chen, M. P. Aldred, Z. Hu, T. Chen, Z. Huang, X. Meng and M.-Q. Zhu, *Chem. Commun.* 2014, **50**, 12058; (b) G.-F. Zhang, Z.-Q. Chen, M. P. Aldred, Z. Hu, T. Chen, Z. Huang, X. Meng and M.-Q. Zhu, *Chem. Commun.*, 2014, **50**, 12058-12060; (c) Q. Qi, J. Zhang, B. Xu, B. Li, S. X.-A. Zhang and W. Tian, *J. Phys. Chem. C*, 2013, **117**, 24997-25003.
- B. Kupcewicz and M. Małacka, *Cryst. Growth Des.*, 2015, **15**, 3893-3904.